RT SOLUTIONS, Inc.
9 Channing Street, Cambridge, MA 02138.

Final Report
O3SAF-VS, 2006

GOME-2 retrievals over the ocean: Forward model simulations using a coupled atmosphere-ocean model

Robert J. D. Spurr

Director, RT Solutions, Inc.
9 Channing Street, Cambridge, MA 02138

25 February 2007

Co-Investigators

Knut Stamnes, Wei Li
Light and Life Laboratory, Stevens Institute for Technology
Castle Point on Hudson, Hoboken, NJ 07030, USA

Co-ordinators (SAF Project)

Diego Loyola
German Aerospace Center,
PO Box 1116,
D82234 Wessling, Germany

Contractual
Jukka Kujanpaa
Finnish Meteorological Institute,
P.O.BOX 503, FIN-00101 Helsinki, Finland

RT Solutions, Inc.
9 Channing Street, Cambridge, MA 02138, USA
Email: rtsolutions@verizon.net

Tel: +1 617 492 1183
Fax: +1 617 354 3415
EIN: 20 1995227

GOME-2 retrievals over the ocean: forward model simulations using a coupled atmosphere-ocean model

1. Introduction

This Final Report summarizes work done under a small 2006 O3M SAF Visiting Scientist (VS) grant to carry out an investigation of forward model errors sources in retrievals of trace gas columns and other atmospheric quantities over the ocean from the GOME-2 Atmospheric Chemistry Instrument. O3SAF funding in 2006 was reduced compared with previous years, and this study is the result of about four weeks of effort by PI Robert Spurr (RT Solutions Inc.) with assistance from co-Is Knut Stamnes and Wei Li (Stevens Institute).

Previous VS activity by PI Robert Spurr has contributed in a major way to the LIDORT development; this includes LIDORT Versions 2.1 and 2.3 (VS 2000 and VS 2001), LIDORT-RRS and LIDORT V2.4 (VS 2002), LIDORT 2.2+ (VS 2003), and the vector model VLIDORT (VS 2004 and VS 2005).

The GOME-2 instrument (on board METOP-1) was launched successfully on October 19th 2006 from the Baikonur proving grounds. At the time of writing, the ground segment is involved with the establishment and proper functioning of the satellite platform and its instruments. First scientific results from the commissioning phase are expected by summer 2007. Like its predecessor GOME-1, GOME-2 has four linear array detectors; these four channels range from 240 to 800 nm with moderate spectral resolution, and there are a number of polarization measurement devices.

There is growing interest in the atmospheric remote sensing community concerning the effect of the oceanic medium on the accuracy of atmospheric retrievals from space. For all GOME-2 retrievals (ozone profiles, trace gas total column amounts, UV index, AAI, cloud properties, etc.) based on the use of polarization-corrected Level 1b total intensity measurements, the water is typically treated as a dark surface with Lambertian albedo of ~2%. Neglect of the absorption and scattering of light in the marine environment can be a significant source of radiance and retrieval error in the UV and visible.

The main purpose of the present work is to carry out an initial study using a coupled atmosphere-ocean radiative transfer model to investigate the consequences of this assumption on simulated satellite radiances. This work sets the stage for further studies quantifying the impact of ocean reflectance on backscatter-based retrievals from GOME-2 and other UV-visible remote sensing instruments, including the role of rough surface scattering as well as inelastic processes.

In this work, simulations of backscatter radiances for GOME-2 are done using the coupled atmosphere-ocean discrete ordinate radiative transfer code (CAO-LDISORT). In Section 2, we summarize the CAO-LDISORT model, and in section 3, we describe the optical models for the atmosphere and ocean. Section 4 sets up the study and presents some initial results.

2. The CAO-LDISORT model

This model was originally developed by Knut Stamnes and co-workers as an extension of the DISORT code [1-3]. The CAO-LDISORT model has been demonstrated to give accurate results in a computationally efficient manner, and it has been validated against Monte-Carlo results [4]. The code has been used extensively in recent work on MODIS ocean color retrievals [5-7], and

has recently been given a complete linearization treatment [8]. The linearized code is fully compatible with the LIDORT and VLIDORT [9-12] radiative transfer models.

The atmosphere and water are regarded as adjacent plane-parallel media separated by an air-water interface, with index of refraction $m_r = 1$ in air and $m_r = 1.34$ in water. Reflection by and transmission through the interface are determined by Fresnel's equations and Snell's law. Each medium is divided into separate optically uniform layers in order to resolve variation of optical properties with altitude/depth. The RT equation is solved separately for each layer using the discrete-ordinate method, and the solution completed by applying boundary conditions at the top of the atmosphere and bottom of the water, including also continuity conditions at the air-water interface (Fresnel's equations) and intermediate layer interfaces. Source function integration yields output at arbitrary viewing angles.

Recent developments concerning this code are also of relevance. The model now has a pseudo-spherical treatment [8], suitable for high solar zenith angle (SZA) nadir viewing scenarios, for which the plane-parallel assumption is not accurate. Solar beam attenuation (before primary scatter) is assumed to take place in a curved spherical shell atmosphere. All multiple scattering is plane-parallel. Curvature may be neglected in the ocean (the maximum SZA in water is 48.75º for refractive index 1.34). The CAO-LDISORT model can also be used in an "enhanced sphericity" environment (viewing paths additionally in a curved atmosphere) suitable for wide-angle off-nadir viewing (a requirement for GOME-2).

CAO-LDISORT has the capability to generate a complete range of weighting functions with respect to any layer atmospheric or oceanic quantity [8]. This makes CAO-LDISORT suitable for use in classical non-linear iterative inversion schemes requiring repeated calculations of simulated radiances and Jacobians. The simultaneous retrieval of atmospheric aerosol quantities and marine chlorophyll and CDOM amounts from MODIS and SeaWiFS radiance measurements has now been demonstrated using this technique [13], and an initial error analysis drawn up for this retrieval [14].

The model is monochromatic; for each wavelength, and for each layer, we require the inherent optical property (IOP) inputs $\{\Delta,\omega,\beta_l\}$, where Δ is the layer optical thickness for extinction, ω the total single scattering albedo, and β_l the set of Legendre expansion coefficients for the total phase function. The user must specify these inputs before calling the model. For the atmosphere, these inputs depend on trace gas distribution profiles and absorption cross-sections, and on molecular scattering and aerosol properties. In the ocean we use a bio-optical model to derive optical properties from intrinsic optical attributes of marine constituents (chlorophyll concentration, yellow stuff, pure water properties). For the linearized model, we require derivatives of the atmosphere and/or ocean IOP inputs.

In this study, we do not consider rough-surface air-water interface effects, inelastic scattering (fluorescence, vibrational Raman scattering by water) and polarization of the oceanic medium. Models to include these effects have now been completed by the present team, and will be considered in a future study; see remarks in section 5.

3. Optical Models for GOME-2 over the ocean

3.1 Atmospheric Model

For each atmospheric layer, we have Rayleigh scattering optical depth σ_{Ray}, molecular absorption optical depth α_{gas}, aerosol extinction and scattering optical depths Δ_{Aer}, and σ_{Aer}. Then the *total optical property inputs* are given by [8]:

$$\Delta = \alpha_{gas} + \sigma_{Ray} + \Delta_{aer}; \quad \omega = \frac{\sigma_{aer} + \sigma_{Ray}}{\Delta}; \quad \beta_l = \frac{\beta_{Ray,l}\sigma_{Ray} + \beta_{aer,l}\sigma_{aer}}{\sigma_{Ray} + \sigma_{aer}}. \tag{1}$$

For aerosols in the marine layers, we use a 2-parameter bimodal model with IOPs defined in terms of the total aerosol number density N_{aer} and the fractional weighting f between the two aerosol modes:

$$\Delta_{aer} = N_{aer} e_{aer} \equiv N_{aer}[\, f e_1 + (1-f) e_2\,]; \tag{2a}$$

$$\omega_{aer} = \frac{\sigma_{aer}}{e_{aer}} \equiv \frac{f z_1 e_1 + (1-f) z_2 e_2}{e_{aer}}; \tag{2b}$$

$$\beta_{l,aer} = \frac{f z_1 e_1 \beta_l^{(1)} + (1-f) z_2 e_2 \beta_l^{(2)}}{\sigma_{aer}}. \tag{2c}$$

Here, e_1, z_1 and $\beta_l^{(1)}$ are the extinction coefficient, single-scattering albedo and phase function expansion coefficients for aerosol type 1 ("fine-mode"), with e_2, z_2 and $\beta_l^{(2)}$ the corresponding values for aerosol type 2 ("coarse-mode"). The fine mode (known as "Tropospheric 50" [6]) comprises 70% water soluble and 30% dust-like particles, with densities 1.85 and 2.7 respectively, with a log-normal distribution having mode radius 0.027 Microns, standard deviation 0.35, and maximum and minimum radii 20 and 0.005 Microns. The coarse mode ("Oceanic 99") comprises 100% sea salt with density 2.45, with a log-normal distribution having mode radius 0.16 Microns, standard deviation 0.40, and maximum and minimum radii 20 and 0.005 Microns. A set of optical properties was calculated at 20 nm intervals from 250 to 810 nm using a Mie program adjusted for humidity. Fractional amounts of the coarse sea-salt mode are small: we use values of 0.995 and 0.999 for the fine-mode weight. For other layers in the atmosphere we use background aerosols from the Lowtran model [15].

3.2 Bio-optical ocean model

In the ocean, the layer total optical depth Δ, the total single scattering albedo ω and phase function Legendre moment coefficients β are given by:

$$\Delta = d\left(\alpha_{water} + \sigma_{water} + \alpha_{chlor} + \sigma_{chlor} + \alpha_{cdom}\right); \tag{3a}$$

$$\omega = \frac{d\left(\sigma_{water} + \sigma_{chlor}\right)}{\Delta}; \; \beta = \frac{\sigma_{water}\beta_{water} + \sigma_{chlor}\beta_{chlor}}{\sigma_{water} + \sigma_{chlor}}. \tag{3b}$$

Here, α_{water} and β_{water} are the pure water absorption and scattering coefficients in [m^{-1}], d is the layer depth in [m]. We assume the following power-law parameterization for chlorophyll absorption in terms of the concentration C [$mg.m^{-3}$]; this is due to Morel [16] as quoted in the book by Mobley [17]:

$$\alpha_{chlor} = a_1 a^+(\lambda) C^{a_2}$$

Here, a_1 = 0.06, with a_2 = 0.65. The chlorophyll-specific absorption coefficients $a^+(\lambda)$ are normalized to the peak value at 440 nm and taken from data by Morel and Maritorena [18].

Scattering coefficients for Chlorophyll are taken from Haltrin and Kattawar [19], again as quoted in Mobley [17]. For β_{chlor}, we start from the well-known data from Petzold [20], creating Legendre-function expansion coefficients using the moment fitting program of Hu et al. [21]. There is also an option to use the Fourier-Forand (FF) phase function (see for example [22]), with the Junge exponent set to 1.08. Again, the moment fitting program is used to create Legendre expansion coefficients.

Refractive indices for water are taken from tables specified in Mobley's book (chapter 3). The pure water phase function is Rayleigh with depolarization ratio 0.0899.

CDOM absorption is given in terms of absorption coefficient Y at wavelength λ_0 (443 nm), via a typical exponential-decay parameterization. Thus:

$$\alpha_{cdom} = Y \exp[-Q(\lambda - \lambda_0)] . \quad (4)$$

The CDOM parameter Q has the value 0.014, and Y is taken to be 0.02 [m^{-1}].

4. Study set-up and initial results

4.1. Atmosphere and ocean profiles

A 22-layer atmosphere is used in the modeling, with resolution 0.5 km in the marine boundary layer, 1.0 km up to 12 km, 2.0 km from 12.0 to 20.0 km, and a coarser spacing up to the top-of-atmosphere level at 60 km. Temperature and pressure profiles are taken from the USA atmospheres [23], and interpolated to this grid. For trace gas absorption, we consider O_3 and NO_2 absorption across the entire GOME-2 spectral range (240 to 790 nm). In the absence of *published* GOME-2 flight model cross-section data, it is sufficient to use a complete set of flight model absorption cross sections from GOME-1 [24, 25]. These are specified at 5 temperatures for O_3 and 3 for NO_2. Data are spline-interpolated to the GOME-2 wavelength grids, then linearly interpolated by temperature.

We use the dynamical column-classified ozone profile climatology prepared for the GOME project [26], with the profile selection based on latitude and time of year and total column amount. The resulting "Umkehr" profile (partial columns in [DU]) is interpolated to the height grid used for modeling. A single NO_2 volume mixing ratio profile is taken from the USA data [23]. Rayleigh cross-sections and depolarization ratios are taken from a recent reappraisal [27].

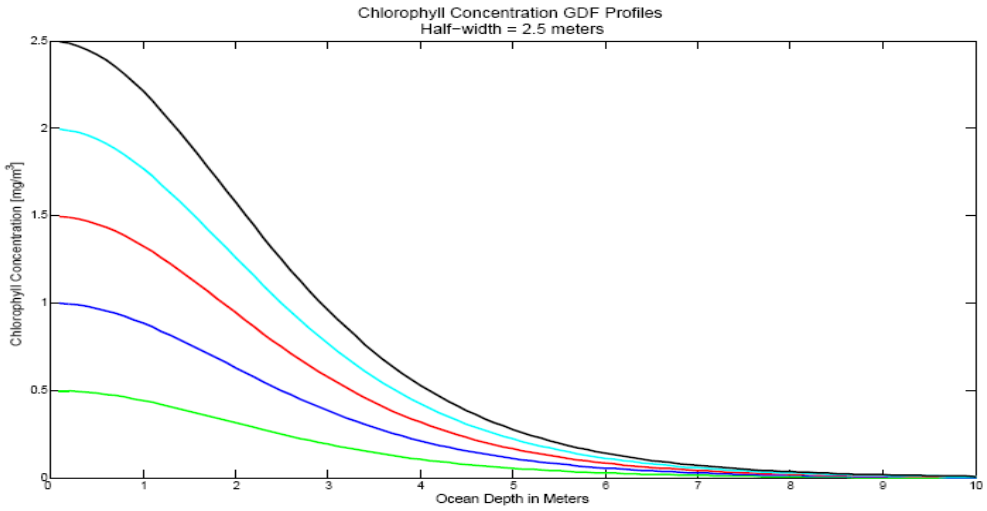

Figure 1. Chlorophyll concentration profiles based on a generalized distribution function.

Rather than assume only the top one or more layers to possess marine constituents, we model the Chlorophyll concentration using a generalized distribution function:

$$C(z) = \frac{4C_0 e^{-sz}}{\left(1+e^{-sz}\right)^2}, \qquad s = \frac{\ln\left(3+\sqrt{8}\right)}{H}. \tag{5}$$

This simple parameterization allows us to control the concentration fall-off with optical depth in a convenient manner. The maximum concentration C_0 occurs at the surface $z = 0$, and the half-width H of the distribution determines the shape of the profile. In the ocean, we used 12 layers down to a depth of 20 meters, with a moderately fine depth resolution in the first 2 meters. Figure 1 shows some profiles for a half-width of 2.5 meters. Our results were done for 10 values of C_0 in [mg.m^{-3}] (0.1, 0.2, 0.4, 0.7, 1.0, 1.5, 2.0, 3.0, 5.0 and 10.0), and for a "black" sea in which the value of C_0 is set to be so high that the surface is effectively a reflecting surface. A similar distribution is used for the CDOM absorption profile, with the surface value Y_0 = 0.02 [m^{-1}] as noted above.

4.2. GOME-2 wavelength settings

We have performed runs at all GOME-2 wavelengths for Channels 2, 3, and 4 as specified in the complete data set of slit functions computed at RAL and provided for this study by S. Slijkhuis (private communication). [Due to lack of data for chlorophyll absorption, calculations for Channel 4 were terminated at 700 nm]. We used the Kitt-Peak spectrum [28] as the reference for a solar spectrum. This was convolved to the GOME-2 wavelengths using the slit function data as noted above.

Note that the slit function shape is specified uniquely by 141 points at each wavelength, although parameters for fitted functions (Gaussians) are provided as ancillary data. Slit functions are specified at points within ±0.7 nm of a pixel wavelength for channels 1 and 2 and within ±1.4 nm of the assigned wavelength in Channels 3 and 4. Convolution of the Kitt Peak spectrum is shown in Figure 2.

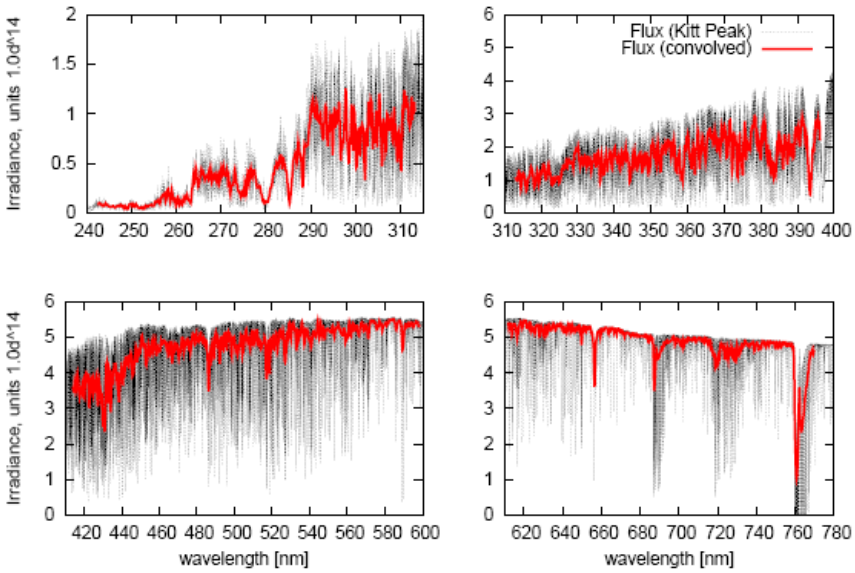

Figure 2. GOME-2 Slit function convolution of the Kitt-Peak solar spectrum.

4.3. Initial results for Channels 2, 3 and 4

Initial results were prepared for three solar zenith angles (33°, 49° and 65°) and 9 viewing zenith angles (from 0° to 40°) in the principal plane (relative azimuth 0°). Ten discrete ordinates were used in the polar hemisphere in the atmosphere and illuminated part of the ocean, with an additional eight streams in the total reflection regime of the ocean. Marine aerosol and chlorophyll scattering are both strongly peaked in the forward direction, and it is necessary to use the delta-M approximation to handle the corresponding Legendre phase function expansions. The plane parallel approximation was used in the atmospheric medium; this is sufficiently accurate for this initial study with the three solar angles as noted above, but it is certainly possible to extend the study to solar zenith angles up to 90 degrees using the pseudo-spherical treatment in the atmosphere [8].

In all cases, we compare results obtained with a variety of chlorophyll concentration profiles with those calculated with a dark surface (no effective Fresnel transmittance). Chlorophyll profiles were established using the parameterization in terms of surface concentrations as noted above in section 4.1.

Figures 3-5 show intensity differences to the dark surface case for the three GOME channels 2, 3 and 4 respectively. Water absorption and scattering are present at all wave wavelengths, so there is always some difference to the dark surface case, no matter what the chlorophyll concentration. Differences are larger for the smaller solar zenith angles (for which more light penetration into the ocean is evident). The overall difference decreases as we go to longer wavelength in channel 4 (Figure 5), where water absorption becomes increasingly substantial. Indeed, the ocean is treated as a dark surface for near infrared channels (for example, 865 nm) in MODIS-type retrievals of ocean color. It is interesting to note that the chlorophyll absorption peak around 675 nm shows up as a leveling feature in the wavelength profiles (Figure 5).

GOME-2 retrievals over the ocean: forward model simulations using a coupled atmosphere-ocean model

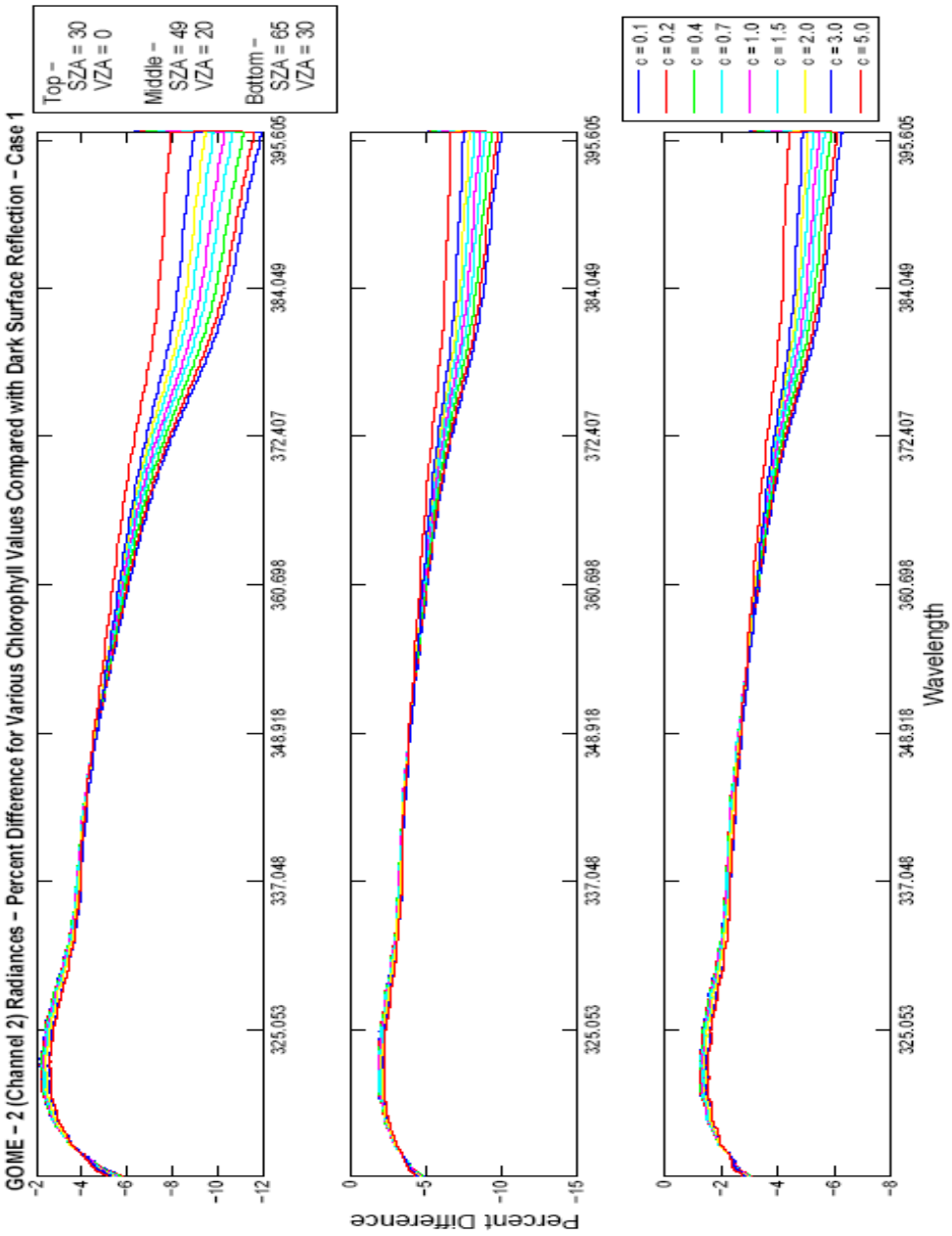

Figure 3. Channel 2 GOME-2 sun-normalized radiances for 9 phytoplankton profiles (surface chlorophyll values as indicated). Results plotted are percentage differences to values corresponding to a dark surface with no Fresnel transmittance. Solar and viewing zenith angles for three scenarios are as indicated in the legend.

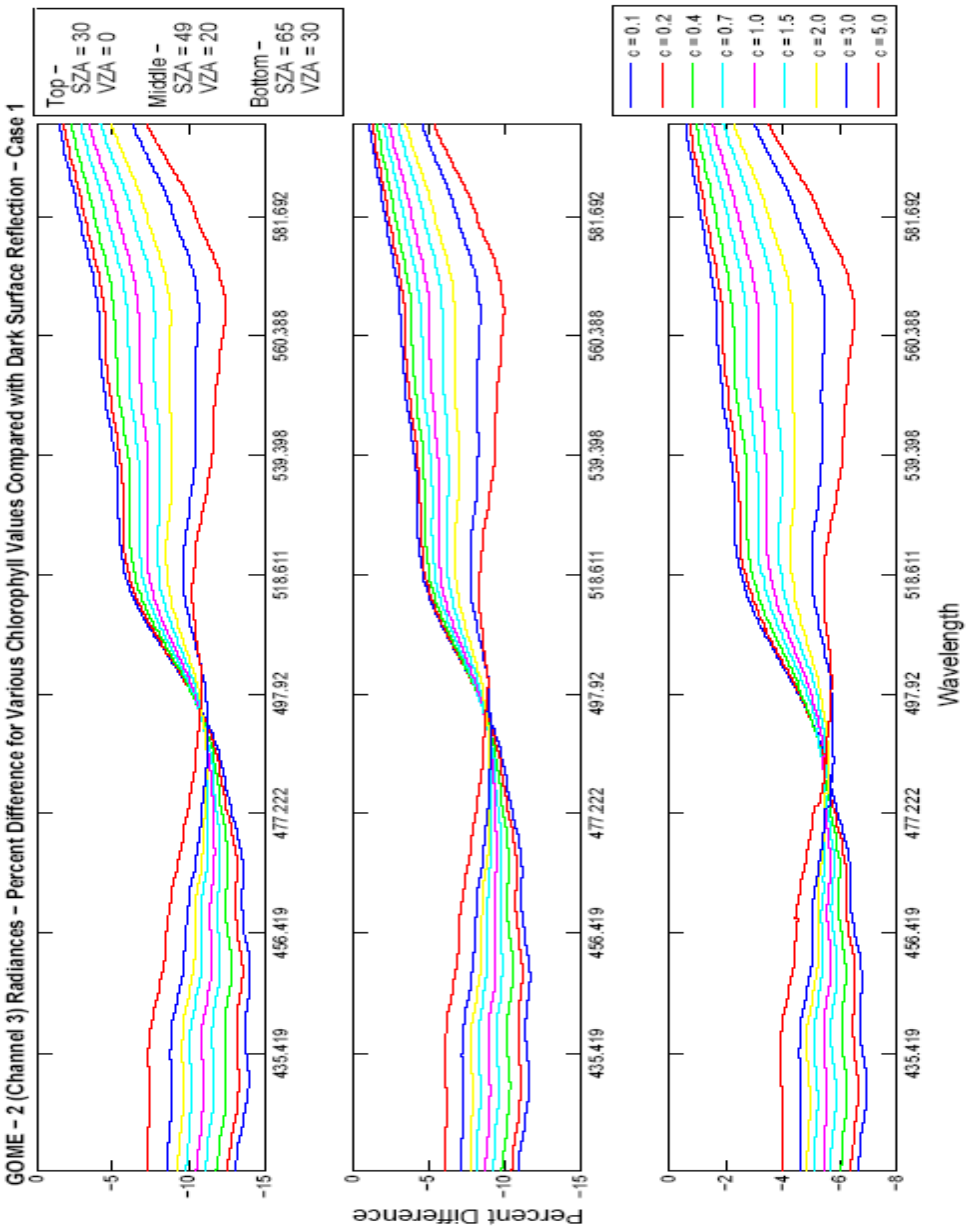

Figure 4. Channel 3 GOME-2 sun-normalized radiance differences to the dark surface case. Solar and viewing angles and range of phytoplankton profiles as in previous figure.

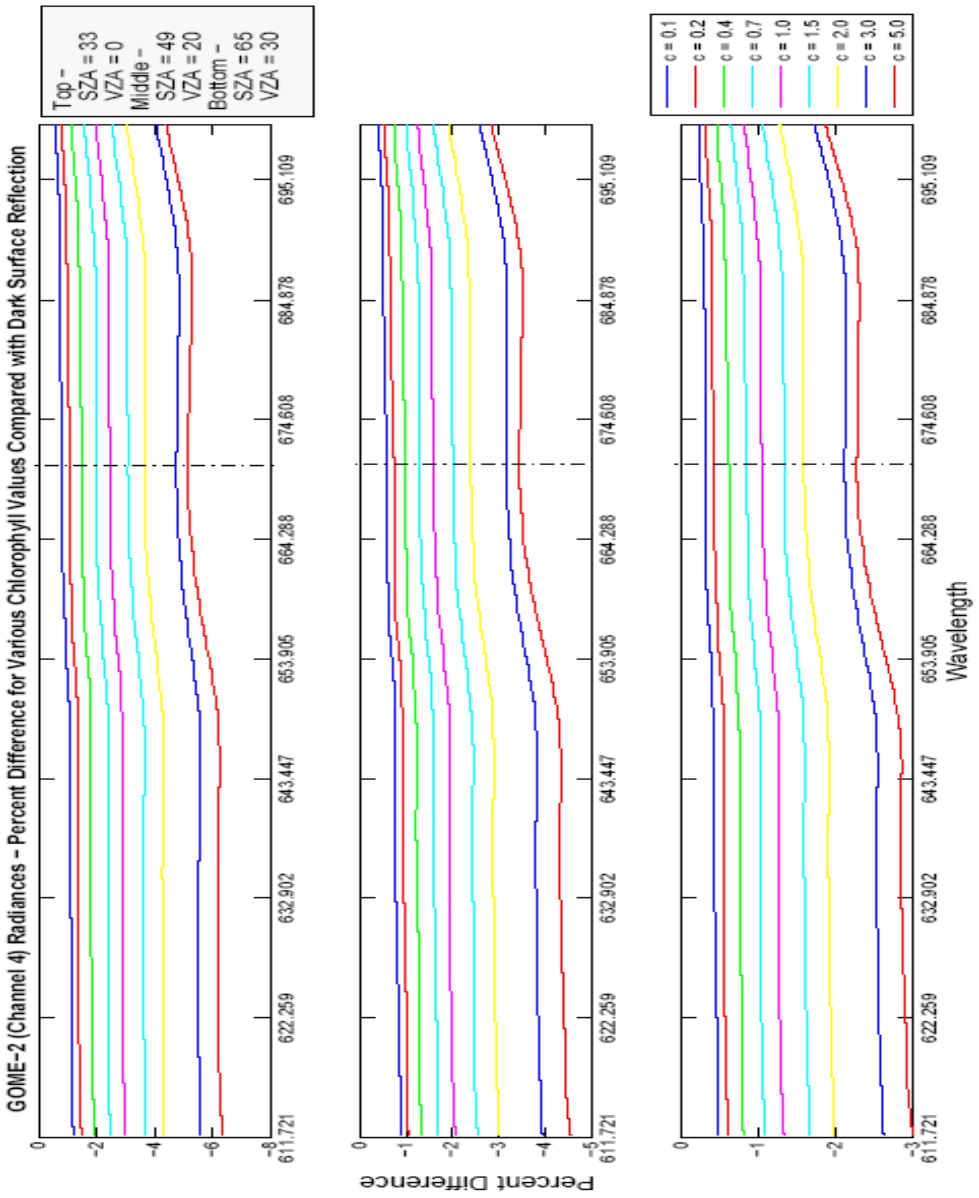

Figure 5. Channel 4 GOME-2 sun-normalized radiance differences for 9 phytoplankton profiles and solar/viewing scenarios as in previous figure. Dotted line at 670 nm denotes the position of the peak of the chlorophyll fluorescence.

Chlorophyll content has little effect in the UV channel (Figure 3), where oceanic effects below about 360 nm are dominated by water absorption and scattering. Standard ozone profile and column retrieval algorithms for GOME-2 are not expected to be strongly affected by ignoring the ocean in the retrieval. Chlorophyll absorption becomes significant as we approach the visible, and the region from 400 to 480 nm has the largest differences. Water absorption is very low here, and increasing chlorophyll concentrations leads to more opacity. There is an interesting reversal in the intensity difference pattern at around 480 nm. Although the level of chlorophyll absorption is falling off at this point, the reasons for this reversal are not clear.

It is clear that ocean effects could affect column retrievals of NO_2 absorption (420-450 nm). The DOAS algorithm for this species relies on highly resolved absorption features from atmospheric NO_2, and ocean effects would be subsumed in the low-order filtering polynomial customarily used to deal with continuum effects. The effect of Raman scattering by water in the ocean is of more significance in this regard [29], and some initial investigations of this effect have been made using simplified hydrological modeling [30].

5. Concluding Remarks

We have developed a new forward model tool for the investigation of simulated GOME-2 radiances using a coupled ocean-atmosphere radiative transfer model. Our initial study was carried out for a limited range of satellite geometries, and a few choices of the controlling marine aerosol and chlorophyll concentration parameters. We have examined the magnitude of the forward model error assumed by supposing the ocean to be a dark reflecting surface.

Further forward modeling extensions will expand the range of these simulations. A new supplement to the coupled atmosphere-ocean model to include inelastic effects from Raman-scattering and fluorescence has just been completed, and this will used in 2007 to investigate these effects for NO_2 GOME-2 retrievals over the ocean. Also newly completed is a fully linearized *rough-surface coupled model* with the ability to carry out simulations in the presence of a wind-driven sea surface.

It is worth noting that these coupled models are fully linearized and are therefore suitable for different retrievals appropriate to the GOME-2 instrument, in which the forward modeling is to be done using proper optical treatment of the ocean. Once we have established the magnitude of forward model errors, we can determine the effect on the retrieved accuracy of trace gas columns and profiles and other products from GOME-2 coming on line in the near future.

6. References

[1] Z. Jin, and K. Stamnes, Radiative transfer in nonuniformly refracting media such as the atmosphere ocean system, *Applied Optics*, **33**, 431-442, 1994.

[2] B. Yan, and K. Stamnes, Fast yet accurate computation of the complete radiance distribution in the coupled atmosphere ocean system, *J. Quant. Spectrosc. Radiat. Transfer* **76**, 207-223, 2003.

[3] G. E. Thomas, and K. Stamnes, *Radiative Transfer in the Atmosphere and Ocean*, Cambridge University Press, 1999.

[4] K. I. Gjerstad, J. J. Stamnes, B. Hamre, J. K. Lotsberg, B. Yan and K. Stamnes, Monte Carlo and discrete-ordinate simulations of irradiances in the coupled atmosphere-ocean system, *Applied Optics*, **42**, 2609-2622, 2003.

[5] B. Yan, K. Stamnes, W. Li,B. Chen, J. Stamnes, and S. C. Tsay. Pitfalls in atmospheric correction of ocean color imagery: How should aerosol optical properties be computed? *Applied Optics*, 42, 412-423, 2003.

[6] K. Stamnes, W. Li,, B. Yan, H. Eide, A. Bernard, W. Pegau, and J. Stamnes, Accurate and self-consistent ocean color algorithm: simultaneous retrieval of aerosol optical properties and chlorophyll concentrations, *Applied Optics*, **42**, 939-951, 2003.

[7] Zhang, K., W. Li, K. Stamnes, H.Eide, R. Spurr and S.-C. Tsay, Assessment of the MODIS algorithm for the retrieval of aerosol parameters over the ocean, *Applied Optics*, in press, 2006.

[8] Spurr, R., K. Stamnes, H. Eide, W. Li, K. Zhang, and J. Stamnes, Simultaneous Retrieval of Aerosols and Ocean Properties: A Classic Inverse Modeling Approach. I. Analytic Jacobians from the Linearized CAO-DISORT Model, *J. Quant. Spectrosc. Radiat. Transfer*, doi: 10.1016/j/jqsrt.2006.09.009 (2006).

[9] Spurr, R.J.D., T.P. Kurosu, and K.V. Chance, A linearized discrete ordinate radiative transfer model for atmospheric remote sensing retrieval, *JQSRT*, **68**, 689-735, 2001.

[10] Spurr, R.J.D., Simultaneous derivation of intensities and weighting functions in a general pseudo-spherical discrete ordinate radiative transfer treatment, *JQSRT*, **75**, 129-175, 2002.

[11] Spurr, R. J. D., A New Approach to the Retrieval of Surface Properties from Earthshine Measurements, *JQSRT*, **83**, 15-46, 2004.

[12] Spurr, R. J. D., VLIDORT: A linearized pseudo-spherical vector discrete ordinate radiative transfer code for forward model and retrieval studies in multilayer multiple scattering media, *J. Quant. Spectrosc. Radiat. Transfer*, 102(2), 316-342, doi:10.1016/j/jqsrt.2006.05.005 (2006).

[13] Spurr, R., K. Stamnes, H. Eide, W. Li, K. Zhang, and J. Stamnes, Simultaneous Retrieval of Aerosols and Ocean Properties: A Classic Inverse Modeling Approach. II. Improved retrievals and a comprehensive error analysis for SeaWiFS ocean color. Paper in preparation (2007).

[14] Spurr, R., K. Stamnes, H. Eide, W. Li, K. Zhang, and J. Stamnes, Error Analysis for Simultaneous Retrieval Of Marine and Aerosol Properties from SeaWiFS Measurements. Ocean Optics XVIII, Montreal, Canada, October 2006.

[15] Shettle E. P., and R. W. Fenn, Models for the aerosols of the lower atmosphere and the effects of humidity variations on their optical properties, Air Force Geophysics Laboratory, Hanscomb Air Force Base, Mass.1979.

[16] Morel, A. Light and marine photosynthesis: a spectral model with geochemical and climatological implications. *Prog. Oceanogr*., **26**, 63, 1991.

[17] Mobley, C. Light and Water: Radiative Transfer in Natural Waters, Academic Press, San Diego, 1994.

[18] Morel, A., and S. Maritorena, Bio-optical properties of oceanic waters: A reappraisal, *J. Geophys. Res*., **106**, 7163–7180, 2001.

[19] Haltrin, V., and G. Kattawar. Self-consistent solutions to the equation of transfer with elastic and inelastic scattering in oceanic optics: I. Model. *Applied Optics*, **32**, 5356-5367, 1993.

[20] Petzold TL. Volume scattering functions for selected ocean waters, Scripps Inst Oceanogr Visibility Lab 1972; pp.72-78.

[21] Hu, Y., B. Wielicki, B. Lin, G. Gibson, S. Tsay, K. Stamnes, and T. Wong, 2000: Delta-fit: A Fast and Accurate Treatment of Particle Scattering Phase Function with Weighted SVD Least Square Fitting. *J. Quant. Spectrosc. Radiat. Transfer*, **65**, 681-690.

[22] Mobley, C., L. Sundman, and E. Boss, Phase function effects on oceanic light fields, *Applied Optics*, **41**, 1035-1050, 2002.

[23] McClatchey, R., W., Fenn, J. E. A. Selby, F. E. Voltz and J. S. Garing, Optical properties of the atmosphere. AFCRL-72-0497, 108 pp. (NTIS-AD753075], 1972.

[24] Burrows, J., A. Dehn, B. Deters, S. Himmelmann, A. Richter, S. Voigt, and J. Orphal, Atmospheric Remote-Sensing Reference Data from GOME: Part 1. Temperature-dependent absorption cross-sections of NO_2 in the 231-794 nm range, *JQSRT*, **60**, 1025-1031, 1998.

[25] Burrows, J., A. Richter, A. Dehn. B. Deters, S. Himmelmann, S. Voigt, and J. Orphal, Atmospheric remote sensing reference data from GOME: Part 2. Temperature-dependent absorption cross-sections of O_3 in the 231-794 nm range, *JQSRT*, **61**, 509-517, 1999.

[26] Coldewey-Egbers, M., M. Weber, L. N. Lamsal, R. de Beek, M. Buchwitz, and J. P. Burrows, Total ozone retrieval from GOME UV spectral data using the weighting function DOAS approach, *Atmos. Chem. Phys.*, **5**, 1015–1025, 2005.

[27] Bodhaine, B., N. Wood, E. Dutton, and J. Slusser, On Rayleigh optical depth calculations, *J. Atmos. Ocean. Tech.*, **16**, 1854-1861, 1999.

[28] Chance, K., and R. Spurr, Ring effect studies: Rayleigh scattering, including molecular parameters for rotational Raman scattering, and the Fraunhofer spectrum, *Applied Optics*, **36**, 5224-5230, 1997.

[29] Vasilkov, A., J. Joiner, J. Gleason, and P. Bhartia, Ocean Raman scattering in satellite backscatter UV measurements, Geophys. Res. Lett., 10, 2002.

[30] Vountas. M. , A. Richter, F. Wittrock, and J. P. Burrows, Inelastic scattering in ocean water and its impact on trace gas retrievals from satellite data, *Atmos. Chem. Phys*., **3**, 1365-1375, 2003.